Science Advances
AAAS

advances.sciencemag.org/cgi/content/full/5/4/eaav3816/DC1

Supplementary Materials for

Imaging localized neuronal activity at fast time scales through biomechanics

Samuel Patz*, Daniel Fovargue, Katharina Schregel, Navid Nazari, Miklos Palotai, Paul E. Barbone, Ben Fabry, Alexander Hammers, Sverre Holm, Sebastian Kozerke, David Nordsletten, Ralph Sinkus*

*Corresponding author. Email: patz@bwh.harvard.edu (S.P.); ralph.sinkus@inserm.fr (R.S.)

Published 17 April 2019, *Sci. Adv.* **5**, eaav3816 (2019)
DOI: 10.1126/sciadv.aav3816

The PDF file includes:

Other Supplementary Material for this manuscript includes the following:

(available at advances.sciencemag.org/cgi/content/full/5/4/eaav3816/DC1)

Movie S1 (.mp4 format). Video of Hind Limb Electrical Stimulation.

SUPPLEMENTARY MATERIAL

MRE pulse sequence

Details of the MRE pulse sequence are provided here.

SLOW LOOPING STRUCTURE

Motion Encoding Loop (3 values for x, y and z displacement direction)
Traditional MRI Phase Encode Loop (64 phase encode values)
Stimulus Loop (2 values: ON/OFF for experiment or OFF/OFF for "control".)
Mechanical Shear Wave-Phase Loop (10 values: 2 dummy and 8 recorded values)
Slice Loop (9 slices, TR/slice =100ms, Total time for slice loop execution = 0.9s).
Stimulus ON period = t_s = 9.0s
Electrical current pulse frequency f_p = 3Hz

The SLOW stimulus switching data was acquired first chronologically. Because we initially hypothesized that the mechanism behind the observed change in viscoelastic properties was due to a neuro-vascular coupling with a time constant of several seconds, we added 1.8 seconds after each stimulus switch to allow for partial hemodynamic equilibrium to be established. To accomplish this, two extra dummy passes through the slice loop, each taking 0.9s, were implemented by adding two repeat values to the first wave-phase in the mechanical wave-phase loop. In practice, this means that during the 9s stimulus period, data used for the MRE reconstruction was acquired from 1.8 - 9s and hence, none of the SLOW data was acquired in close temporal proximity to the stimulus transient.

FAST LOOPING STRUCTURE

Motion Encoding Loop (3 values for x, y and z displacement direction)
Traditional MRI Phase Encode Loop (64 phase encode values)
Mechanical Shear Wave-Phase Loop (8 values)
Stimulus Loop (2 values: ON/OFF for experiment or OFF/OFF for "control".)
Slice Loop (9 slices, TR/slice =100ms, Total time for slice loop execution = 0.9s).
Stimulus ON period = t_s = 0.9s
Electrical current pulse frequency f_p = 10Hz

Ultra-FAST LOOPING STRUCTURE

Motion Encoding Loop (3 values for x, y and z displacement direction)
Traditional MRI Phase Encode Loop (64 phase encode values)
Mechanical Shear Wave-Phase Loop (8 values)
Combined Stimulus & Slice Loop: (2 stimulus states and 9 slices interleaved as follows:
1 3 5 7 9 2 4 6 8 1 3 5 7 9 2 4 6 8,
numbers correspond to slice number, red/green are the two stimulus states,
TR/slice =100ms, Total time for combined slice & stimulus loop execution = 1.8s.
Stimulus ON period = t_s = 0.1s
Electrical current pulse frequency f_p = 100Hz

For the FAST and Ultra-FAST data acquisitions, the total acquisition time was 46 minutes. This consisted of (9 slices)*(8 wave-phases)*(2 stimulus states)*(3 motion encoding directions)*(64 phase encodes)*(0.1s for each TR/slices) = 46.08 minutes. For the SLOW acquisition, because there were an additional 2 dummy wave-phases, the data acquisition time was 57.6 minutes.

Nine contiguous slices covering 2.7mm and with in-plane field of view of 19.2mm x 19.2mm were acquired. Experiments were performed on a Bruker 7T pre-clinical system with 650mT/m gradient strength. Mechanical vibration to the mouse head was provided by a custom electromechanical actuator delivering 1000Hz vibrations designed to produce shear waves of less than 10μm amplitude through the mouse brain.

For electrical stimulation, short 1.5 – 2mA electrical current pulses of ~250μs duration were used. Because the clock for the stimulation pulses and the scanner clock that switched between ON and OFF stimulation were not phase locked, a variable phase between the two clocks could develop during data acquisition resulting in the stimulation pulses not occurring at exactly the same time points during the stimulation period t_s. To reduce the temporal variation of when the stimulation pulses could occur to no more than 0.1 t_s, the frequency of these pulses f_p was adjusted so that a minimum of 10 pulses were applied during each time t_s. Hence, f_p was 3Hz, 10Hz, and 100Hz for the SLOW, FAST, and Ultra-FAST cases respectively. The current was adjusted using a 3Hz pulse frequency until at least one digit was observed to twitch in synchrony with the pulses (see supplemental video "mouse_digit_twitch.mp4"). The frequency was then increased for the FAST and Ultra-FAST experiments where one could no longer observe individual twitches but rather a fused or tetanic contraction that was constant during t_s.

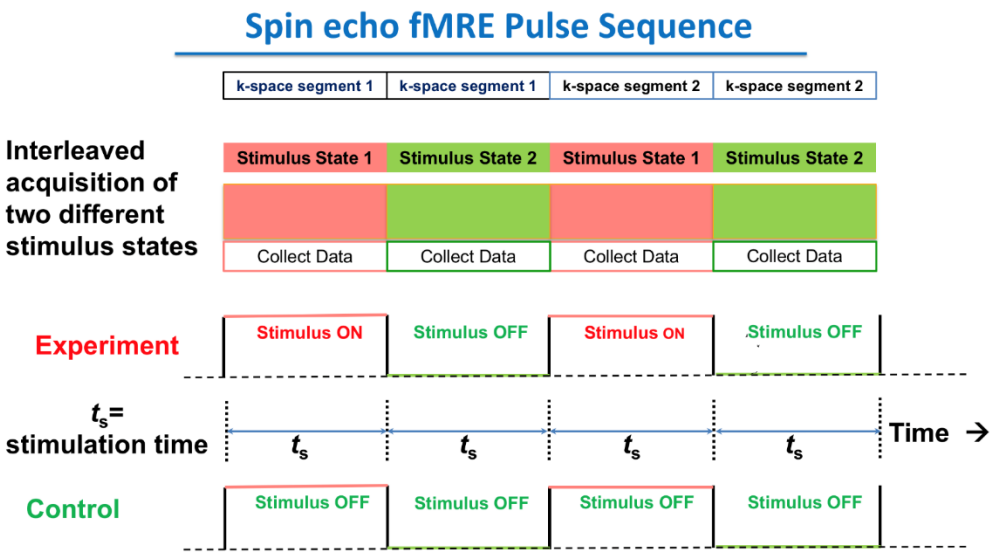

Fig. S1. Schematic of the fMRE pulse sequence.

Animal experimental results

For the three stimulus switching frequencies, SLOW, FAST and Ultra-FAST, a total of 7, 5 and 4 animals were studied respectively. The animals studied in the Ultra-FAST protocol were studied twice, with a minimum of 6 weeks separating each study. A small number of the scans were rejected because of severe artifacts, low SNR, and/or inability to unwrap phase. Those artifacts originated from hardware failures, like mechanical fractures in the 3D-printed plastics parts of the head-rocker. Details are shown in **table S1**. Numerical details for the data shown in Fig. 4E are provided in **tables S2 and S3**.

Table S1. Each animal study included both an experiment and a control scan. Each animal study included both an experiment and a control scan. An experiment scan collected interleaved k-space data for the two stimulation states ON and OFF. The control scan collected interleaved k-space data for two OFF states. Some scans were rejected because of severe artifacts, low SNR, and/or inability to unwrap phase. Note that different mice were used for every study except for the Ultra-FAST protocol where four mice were each studied twice. Any repeat studies were performed at least 6 weeks apart.

	SLOW	FAST	Ultra-FAST
# mice studied (# repeats)	7 (1) = 7 studies	5 (1) = 5 studies	4 (2) = 8 studies
# valid Experiment scans	7	5	6
# valid Control scans	5	4	6

Table S2. Averaged ROI differences. The mean and standard deviation (std) for the purple ROI regions shown in Fig. 4B after they are averaged over the different animal studies. This data corresponds to the filled symbols of Fig. 4E.

ΔG' (kPa)	**SLOW**	**FAST**	**Ultra-FAST**
Experiment Mean (std)	0.81 (0.17)	0.97 (0.17)	0.80 (0.12)
Control Mean (std)	-0.16 (0.21)	0.0025 (0.31)	0.13 (0.16)

Table S3. Individual animal ROI differences. Differences in elastic modulus ΔG' (kPa) between the two stimulus states for experiment and control scans for each animal studied using the purple ROIs shown in Fig. 4B. This data corresponds to that shown in Fig. 4E with open data symbols.

Mouse # Repeat #	1 1	2 1	3 1	4 1	5 1	6 1	7 1	
SLOW Experiment	-0.170	0.188	0.486	0.410	1.833	0.979	1.939	Δ*G*' (kPa)
SLOW Control	-0.034	-0.404	-0.272	-0.179	0.074			Δ*G*' (kPa)
Mouse # Repeat #	1 1	2 1	3 1	4 1	5 1			
FAST Experiment	1.5715	1.684	0.374	0.611	0.614			Δ*G*' (kPa)
FAST Control	0.201	-0.190	0.253	-0.254				Δ*G*' (kPa)
Mouse # Repeat #	1 1	2 1	3 1	4 1	1 2	2 2		
Ultra-FAST Experiment	0.810	1.083	0.398	0.546	1.233	0.716		Δ*G*' (kPa)
Ultra-FAST Control	0.265	-.0851	-0.0354	0.179	0.108	0.335		Δ*G*' (kPa)

The cingulate gyrus region does not include major blood vessels

It is important to note that the region indicated as the cingulate/retrospenial gyrus and identified as a region of activation when switching the stimulus between ON and OFF, does not include major blood vessels. Otherwise, one might speculate that a vascular response is the cause of the change in stiffness, at least for the SLOW protocol. To demonstrate that the major blood vessels in that area, i.e. the superior and inferior sagittal sinus and the internal cerebral veins, are not part of the indicated region of activation, see fig. S2, which shows the location of these blood vessels on the corresponding anatomical T2-weighted scans for the single animal data shown in Fig. 3A.

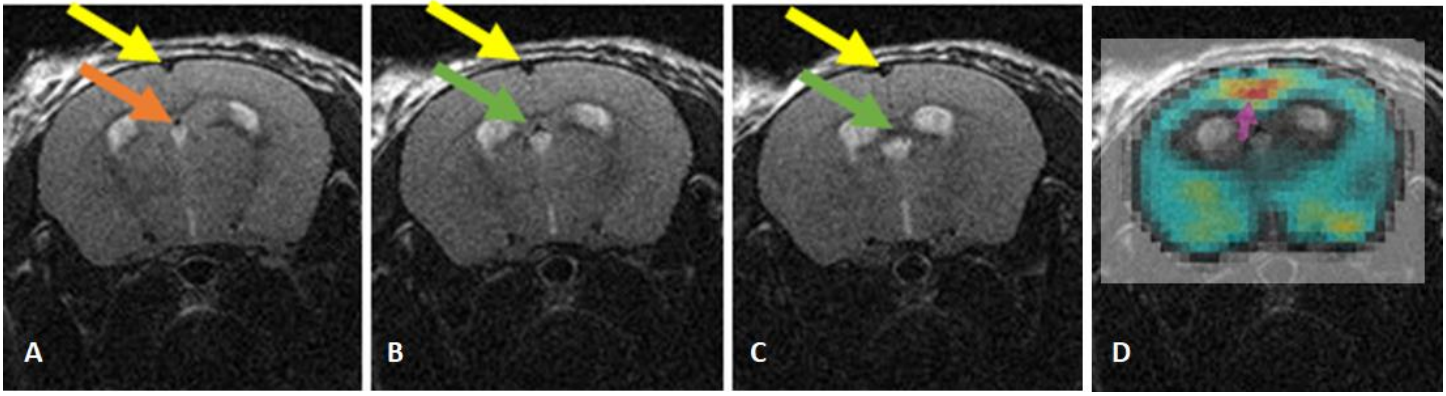

Fig. S2. Location of blood vessels compared to location of stiffness increase in the cingulate/retrosplenial gyrus region. (**A-C**) T2-weighted scans corresponding to the anatomical location of the three slices averaged in the MRE maps to produce the images in Fig. 3A. (**D**) Stiffness map from the Experiment stimulus OFF state overlayed onto the central of these three slices. Note that the region where a change in stiffness is shown (pink arrow) does not correspond to blood vessels as shown by the yellow and orange arrows that indicate the superior and inferior sagittal sinus respectively, or the green arrows that depict the internal cerebral veins.